



HAL
open science

Pattern of Monoclinic Phase Distribution in Nascent UHMWPE Particles

D. Anokhin, K. Grafkskaia, D. Ivanov, E. Ivan'kova, V. Marikhin, L. Myasnikova, S. Ivanchev

► **To cite this version:**

D. Anokhin, K. Grafkskaia, D. Ivanov, E. Ivan'kova, V. Marikhin, et al.. Pattern of Monoclinic Phase Distribution in Nascent UHMWPE Particles. *Physics of the Solid State*, 2020, 62 (8), pp.1493-1499. 10.1134/S1063783420080028 . hal-03095917

HAL Id: hal-03095917

<https://hal.science/hal-03095917>

Submitted on 7 Jan 2021

HAL is a multi-disciplinary open access archive for the deposit and dissemination of scientific research documents, whether they are published or not. The documents may come from teaching and research institutions in France or abroad, or from public or private research centers.

L'archive ouverte pluridisciplinaire **HAL**, est destinée au dépôt et à la diffusion de documents scientifiques de niveau recherche, publiés ou non, émanant des établissements d'enseignement et de recherche français ou étrangers, des laboratoires publics ou privés.

Pattern of Monoclinic Phase Distribution in Nascent UHMWPE Particles

D. V. Anokhina, b, c, K. N. Grafskaiab, c, D. A. Ivanova, d, E. M. Ivan'kovae, V. A. Marikhin f, L. P. Myasnikova f,*,**, and S. S. Ivancheve

A Moscow State University, Moscow, Russia

b Institute of Problems of Chemical Physics, Chernogolovka, Russia

c Moscow Institute of Physics and Technology (MIPT), Moscow, Russia

d Institute of Material Science of Mulhouse, Mulhouse, France

e Institute of Macromolecular Compounds, Russian Academy of Sciences, St. Petersburg, Russia

f Ioffe Institute, St. Petersburg, Russia

*e-mail: liu2000@mail.ru

**e-mail: Liuba.Myasnikova@mail.ioffe.ru

Abstract—By using the ID13 nanofocus beamline of the European Synchrotron Radiation Facility (Grenoble, France), an X-ray diffraction study of a “virgin” particle of ultra-high molecular weight polyethylene (UHMWPE) taken directly from the powder synthesis products and not subjected to any external mechanical action was carried out. The X-ray diffraction curves obtained by scanning a randomly selected region of the particle $100 \times 20 \mu\text{m}$ in size with a $0.3 \times 0.3 \mu\text{m}$ microbeam with a horizontal step of $2 \mu\text{m}$ and vertical step of $0.5 \mu\text{m}$ exhibited reflexes from the metastable monoclinic phase along with reflections from the orthorhombic phase. It can be supposed that it could be caused by the stresses that developed at specific structure formation during slurry synthesis and were preserved at cooling to room temperature and solvent evaporation. The possibility of the monoclinic phase localization in various morphological formations is discussed.

Keywords: reactor powder, ultrahigh-molecular weight polyethylene, synchrotron radiation, microfocus, monoclinic phase

1. INTRODUCTION

In recent years a dry (solvent-free) method for producing high-strength high-modulus filaments directly from the reactor powder (RP) of ultra-high molecular weight polyethylene (UHMWPE), which is an alternative to the expensive and environmentally unsafe method of gel technology, has been intensely developed. Despite the fact that a significant success has been achieved in this area [1–9] and the commercial production of Endumax films (Teijin-Aramid firm) has been started, the strength characteristics of the material produced by the solvent-free method still remain lower (2.5 GPa) than the strengths of commercial UHMWPE fibers Dyneema (DSM, the Netherlands) and Spectra (Honeywell, USA) obtained by the gel technology (3.7–4.7 GPa). To obtain highstrength UHMWPE film filaments by the dry method, a monolithic precursor made from the UHMWPE reactor powder is subjected to a multi-stage orientational drawing at an elevated temperature. The monolithic precursor formation is carried out in two stages (compaction and sintering) which are aimed at healing the boundaries between particles owing to their coalescence and creating cohesive bonds between them that do not allow the precursor to break in the process of orientational hardening (drawing) before it reaches the maximum possible elongation and, hence, acquires high mechanical characteristics. The powder is compacted at room temperature and

is sintered at an elevated temperature, but below the melting temperature, in order to preserve, to a maximum possible extent, the initial structure obtained in polymer synthesis. A key role in obtaining a good precursor for orientational drawing is played by the choice of reactor powder, since, as it is known, not all reactor powders of UHMWPE have good compactability and drawability [10]. To obtain a very high mechanical performance, optimization of the temperature/pressure/ time sintering regime is undoubtedly necessary.

In our previous paper [11] we discussed the problem of the existence of a monoclinic phase (MP) in the UHMWPE RP, the presence of which is regarded by various authors as a criterion for the suitability of a powder for processing into high-performance material by the solvent-free method. The scientific literature gives a lot of data regarding the MP content in nascent UHMWPE. However, there is a huge scatter in the estimates of the MP percentage in powders (from a few percent to 50%) [12, 13]. On the one hand, this can be explained by the fact that the RPs obtained by using various catalytic systems or synthesized under different conditions (stirring speed, gas pressure, solvent, temperature, cocatalyst, etc.) were studied. On the other hand, since the MP can be formed under pressure, the difference in the estimates of the MP content can be caused by various pressures applied at compaction of the powder into tablets used in modern diffractometers to study materials by powder diffraction in the reflection mode. It must be said that even when a "transmission mode" is used, it is impossible to avoid some powder compaction, and this can also lead to the MP formation. The use of high-power synchrotron radiation on the "Belok" line in the National Research Center Kurchatov Institute allowed us [14] to record earlier X-ray diffraction curves from an individual powder particle that was not subjected to any external mechanical stress and to show that the monoclinic phase content in the "virgin" powder particle is much lower than that in a compacted tablet. It was supposed that different mechanisms were responsible for the MP formation during synthesis and compaction. In [15], a comparative analysis of the glow curves of plasma-induced and radiothermoluminescence led to the conclusion that the MP was predominantly localized in near-surface nanolayers of reactor powder particles. Since near-surface layers of particles are involved in the coalescence of particles and the formation of cohesive bonds, it was important to find out how the MP was really distributed in the nascent particle volume. The problem in the analysis of MP localization is that the reactor powder particle has a very developed surface, and particle sizes are tens of micrometers. The optimal method for analyzing the structure of such samples is microfocus X-ray diffraction using synchrotron radiation. As we showed earlier on the examples of various flexible and semi-rigid polymers, this method allows one to determine the phase composition of samples at a scale of micrometers and also to study the structure evolution during ultrafast heating and cooling [16–18]. The goal of our study reported here was to reveal the distribution of the monoclinic phase throughout the particle volume of the UHMWPE reactor powder by using microfocus X-ray diffraction.

2. EXPERIMENTAL

2.1. Materials

The object of the study was an individual (virgin) sufficiently large particle of the UHMWPE reactor powder (UHMWPE RP) selected from the products of slurry polymerization of PE in toluene according to the procedure described in [19] using titanium halide phenoxy-imine catalysts with a special structure activated by methylaluminoxane. The synthesis was carried out at the Institute of Macromolecular Compounds of RAS (St. Petersburg, Russia). The molecular mass of the obtained RP was 3.5×10^6 g/mol, and the green density was 0.065 g/cm³.

2.2. X-ray Studies

Microfocus X-ray diffraction measurements were performed on the ID13 line of the European Synchrotron Radiation Facility (Grenoble, France) at wavelength $\lambda = 0.83$ Å. We scanned an arbitrarily selected region of a particle with a size of (100×20) μm by a (0.3×0.3) μm microbeam with a horizontal step of 2 μm and vertical step of 0.5 μm. The exposure time was 2 s. Two-dimensional diffraction patterns were recorded

by using a Frelon CCD detector. The wave vector modulus s ($s = 2\sin\theta/\lambda$, where θ is the Bragg angle) was calibrated by using several diffraction orders of an α -Al₂O₃ calibrant. Analysis of onedimensional diffraction patterns obtained by integrating two-dimensional diffraction patterns was carried out with the help of a software package created by the authors in the Igor Pro environment (Wavemetrics Inc.).

3. ELECTRON MICROSCOPIC STUDIES

Particles of UHMWPE RP were placed on a conductive adhesive substrate and covered with a 10– 15 nm thick gold layer by cathode sputtering in an EDWARDS Sputter Coater S150B instrument. The study was carried out in a SUPRA55VP-35-49 scanning electron microscope under a voltage of 15 kV. The microscope resolution was 3 nm.

4. RESULTS AND DISCUSSION

Figure 1 shows a micrograph of a PE particle with the scanning area indicated on it (a rectangle marked with white lines). The micrograph size is 576 × 768 pixels (144 × 192) μm , magnification is $\times 50$. The scanning area was 100 × 20 μm (400 × 80 pixels) (200 × 10 points were analyzed in the scanning area). Reflections of both the PE orthorhombic and monoclinic phases were observed on almost all diffraction patterns. One of these diffraction patterns is shown in Fig. 2. The arrows indicate the reflexes of monoclinic and orthorhombic phases and their indices. However, the 2D X-ray diffraction patterns obtained from different points were noticeably different. The difference in the intensities and shapes of the profiles of the X-ray diffraction curves obtained by integrating two-dimensional diffraction patterns is especially pronounced for the points in the particle center (1) and edge (2), see Fig. 3.

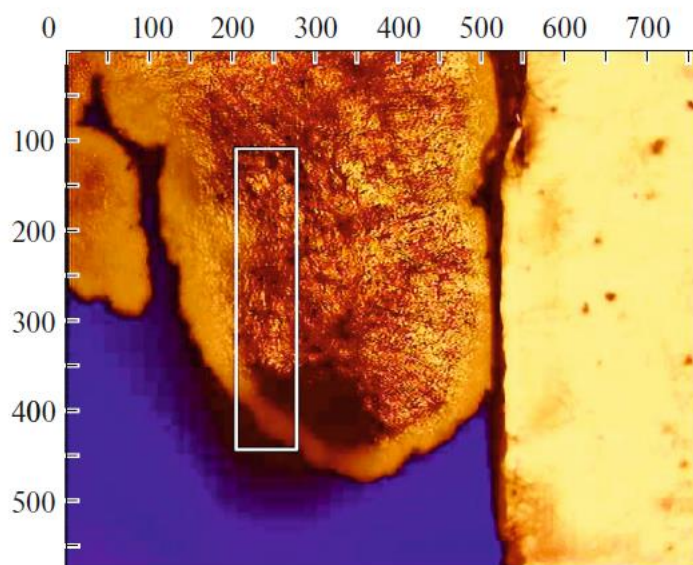


Fig. 1. Micrograph of a PE particle with $\times 50$ magnification with a highlighted (marked) scanning area.

To estimate the contents of mono and orthorhombic phases, it was necessary to decompose the experimental diffraction curves into individual peaks corresponding to these phases. However, when the decomposition of the experimental curves using various profile functions into the peaks corresponding to the most intense reflections of the monoclinic phase (001/200) and orthorhombic phase (110/200) (the intensity of the remaining reflections was extremely low and comparable in scale with the noise) did not give a good agreement between the experimental and fitted curves. This was apparently attributable to the asymmetry of the recorded reflexes which had an instrumental nature caused by the inhomogeneous distribution of intensity over the nanobeam cross section because of its multi-stage focusing. This

assumption is confirmed by the results of fitting of the (012) reflex of the calibrant (α -Al₂O₃). It was found that the peak fitting by three types of symmetric functions (Gauss, Lorenz, Voigt) could not fully compensate for the asymmetry of the reflex. Because of the asymmetry of the X-ray diffraction peaks, which increases with increasing scattering angle, we limited ourselves to the analysis of X-ray diffraction curves for the scattering vector s from 0.21 to 0.26 Å⁻¹. The Voigt profile function was used to approximate the experimental data.

From the results of the analysis, the positions and integral intensities of 001 reflex of the monoclinic phase and 110 reflex of the orthorhombic phase were determined. Due to the overlap of those peaks with 200 reflex for the monoclinic and orthorhombic phases, the fitting of these peaks was difficult and was not carried out. An example of decomposition of the experimental curve into components is presented in Fig. 4. The initial experimental curve was corrected for the Lorentz factor.

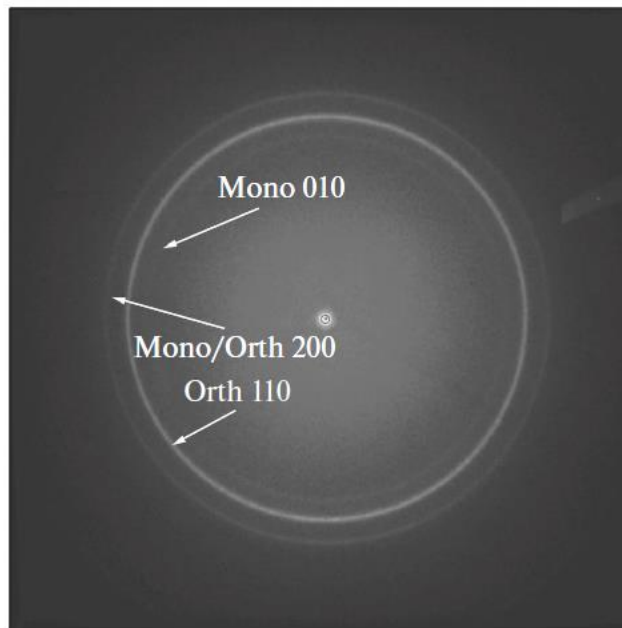


Fig. 2. Two-dimensional diffraction pattern for one of the points of the UHMWPE particle. The arrows indicate the reflexes of the orthorhombic (Orth) and monoclinic (Mono) phases and their indices

To determine the phase composition, a map of the distribution of the monoclinic phase volume fraction was constructed (Fig. 5). The values at each map point were calculated as

$$\Phi_{\text{mon}001} = \frac{V_{\text{mon}001}}{V_{\text{orth}110} + V_{\text{mon}001}} = \frac{\frac{V_{\text{mon}001}}{V_{\text{orth}110}}}{1 + \frac{V_{\text{mon}001}}{V_{\text{orth}110}}},$$

$$\frac{V_{\text{mon}001}}{V_{\text{orth}110}} = \frac{I_{\text{mon}001} (S_{\text{mon}}) F_{\text{orth}110}^2}{I_{\text{orth}110} (S_{\text{orth}}) F_{\text{mon}001}^2},$$

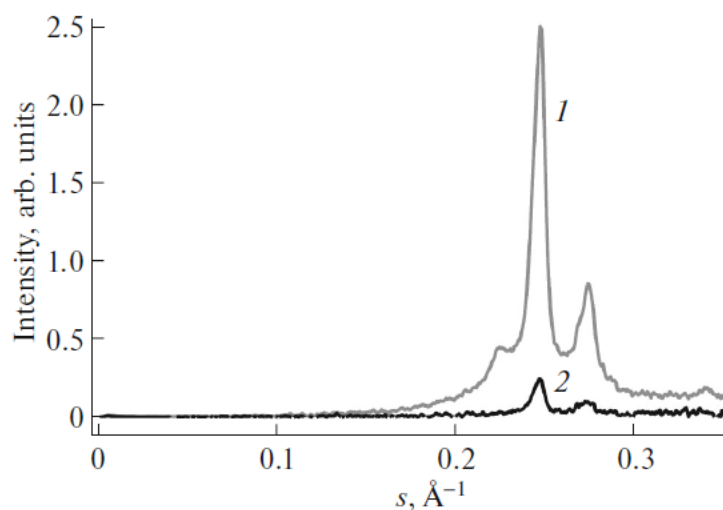


Fig. 3. One-dimensional integral X-ray diffraction curves recorded for the UHMWPE particle center (1) and edge (2).

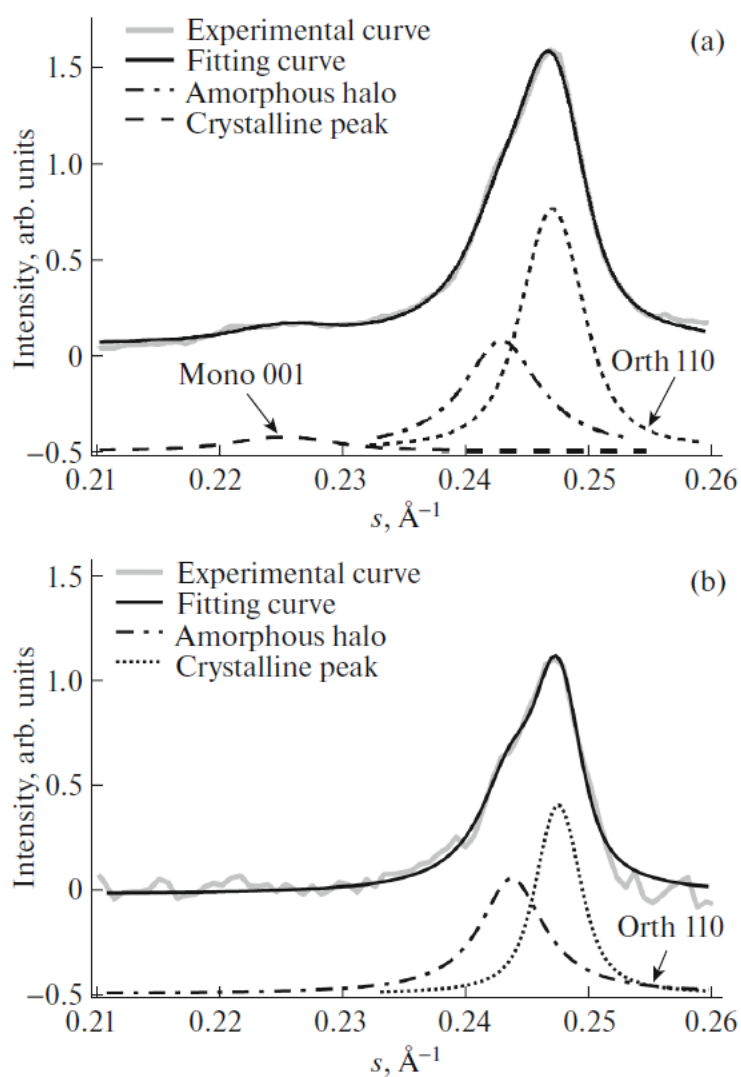


Fig. 4. Example of decomposition of a one-dimensional xray diffraction curve (solid gray curve) into an amorphous halo (black dash-dotted curve), crystalline 001 reflections of the monoclinic phase (black dashed curve) and 110 reflections of the orthorhombic phase (black dashed curve) at the particle center (a) and edge (b). The summary approximation curve is shown by a black solid line.

where \mathbf{h} is the reciprocal lattice vector for the corresponding intensity of the i phase, I_j is the integral intensity j of the reflex of the i phase determined from the fitting results, F_L is the structural factor for the L phase. The structural factor for $L = 16$ [20], for $L = 0.51$ [21]. As can be seen from the map in Fig. 6, the values do not exceed 0.2 over the entire scanning area, which corresponds to 20% of the monoclinic phase content. However, the volume fraction of the monoclinic phase is predominantly from 5 to 15%. Calculations show the absence of a monoclinic phase at the particle edge. However, it cannot be unequivocally stated at present that there are no crystallites of the monoclinic phase at the particle edge. The result obtained is most likely due to a very small amount of the diffracting volume and, as a result, the low intensity of X-ray scattering, which does not allow the monoclinic phase peak to be resolved. At a larger distance from the edge the monoclinic phase distribution over the particle volume is seen to be inhomogeneous. The question arises about the causes of the metastable monoclinic phase formation in the synthesis of ultrahigh molecular weight polyethylene and its localization.

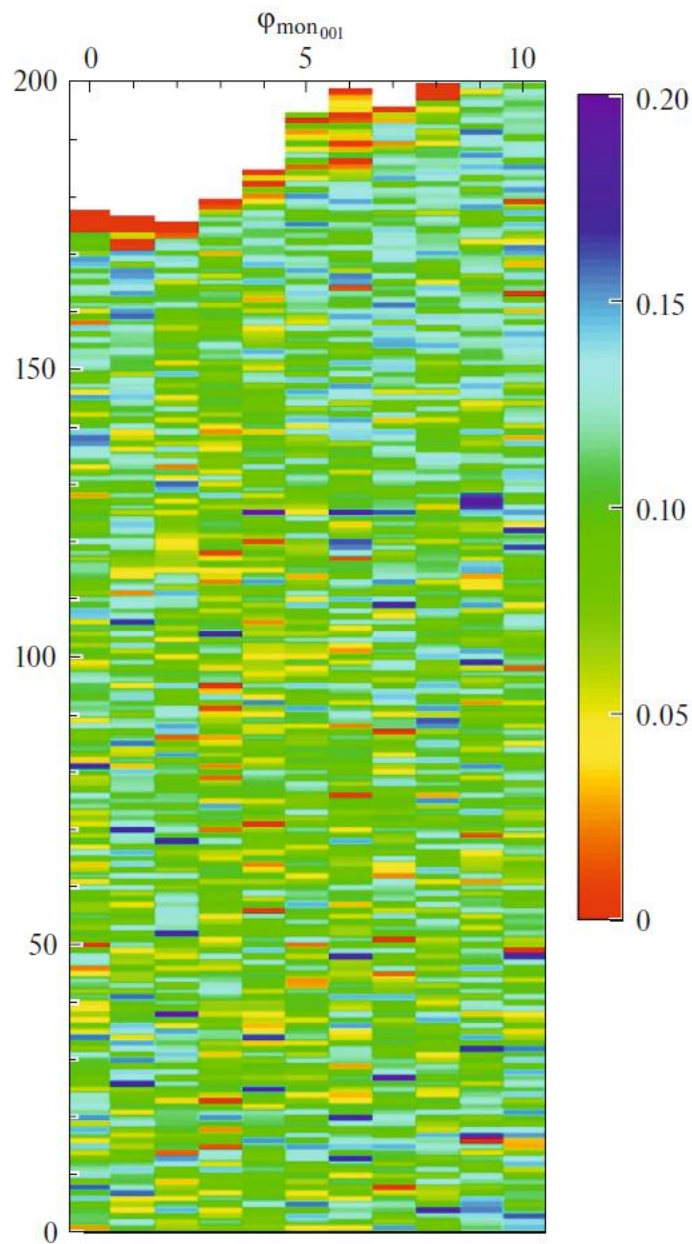


Fig. 5. Distribution map of monoclinic phase volume fraction in the scanned volume of the UHMWPE particle.

In electron scanning electron microscopic images of the particle (Fig. 6) taken at different magnifications (the scale is shown for each image), fibrillar bundles with a shish-kebab type structure can be clearly distinguished along with lamellar morphological units [22]. A separate shish-kebab is clearly visible in the lower right image.

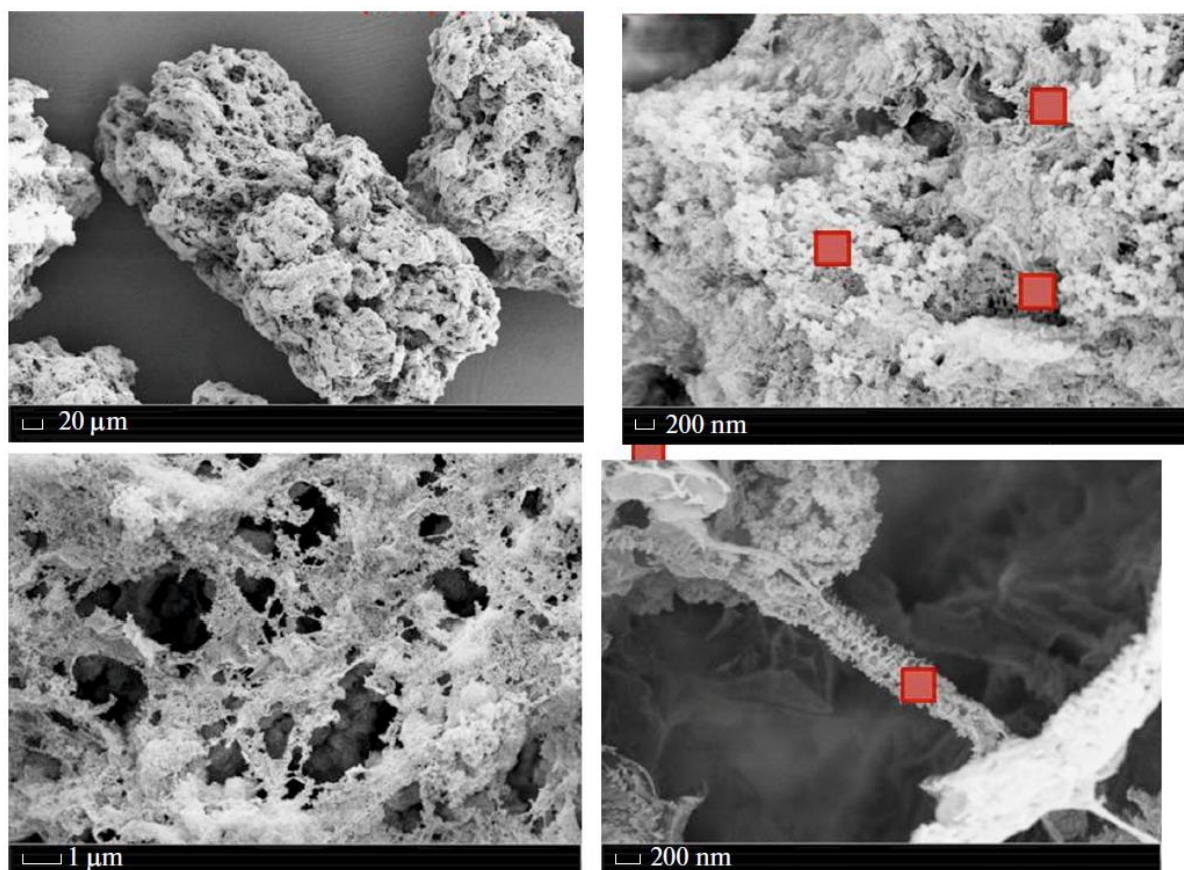


Fig. 6. Scanning electron microscopic images of the UHMWPE particle at different magnifications (the scales are shown in each image, the size of the squares corresponds to the X-ray nanobeam cross section).

If we compare the X-ray beam size with the nonuniformity of the distribution of supermolecular structural units and take into account nanobeam displacement scale, it becomes obvious that it is possible to detect X-ray diffraction from the areas with a predominant localization of fibrillar or lamellar structural elements. Figure 7 schematically shows the conformations of molecular segments in individual structural formations, which have been thoroughly studied by many authors [10, 23–26]. Since the monoclinic phase is stable only when a stress is applied, clusters of taut tie molecular segments passing from one crystallite to another should be sought in disordered regions. Such clusters can be taut molecules in the central region of shish-kebab formations (Fig. 7a) and nanobridges in interlamellar regions (Fig. 7b) that distort a rectangular orthorhombic cell. The idea about the monoclinic phase localization in such areas was already put forward by the authors on the basis of the analysis of differential scanning calorimetry data [27]. However, it is not possible to state with a high certainty at present in what particular areas the monoclinic phase is predominantly formed.

5. CONCLUSIONS

The investigations have led to the conclusion that two crystalline modifications coexist in the UHMWPE reactor powder under study: the orthorhombic and monoclinic ones. The monoclinic phase distribution over the particle volume is inhomogeneous. Its content ranges from 5 to 20%. The comparison of the

beam size with the sizes of lamellar and fibrillar morphological formations that are nonuniformly distributed over the particle volume does not allow us to unequivocally state in what morphological units the monoclinic phase is predominantly localized. It can be supposed that the monoclinic phase can arise both in the central part of fibrillar bundles, such as shish-kebabs, which can be presumably formed under the action of tensile stress generated during the polymer mass growth and in interlamellar nanobridges formed by taut tie molecules. Such a monoclinic phase is stable and remains unchanged with time. It can be classified as a structurally stabilized modification, in contrast to the monoclinic phase formed during plastic deformation of polyethylene due to shear and slip of crystallographic planes.

Fig. 7. Electron microscopic images of shish-kebab (a) and cluster of lamellae (b) and schematic representation of configurations of molecular segments in these supermolecular formations.

CONFLICT OF INTERESTS

The authors declare that they have no conflicts of interest.

REFERENCES

1. P. Smith, H. D. Chanzy, and B. P. Rotzinger, *Polym. Commun.* 26, 258 (1985).
2. Y. L. Joo, H. Zhou, S.-G. Lee, and J. K. Song, *J. Appl. Polym. Sci.* 98, 718 (2005).
3. S. Rastogi, Y. Yao, S. Ponca, van der Eem, and J. Bos, *Macromolecules* 44, 5558 (2011).
4. A. Pandey, Y. Champouret, and S. Rastogi, *Macromolecules* 44, 4952 (2011).
5. S. Ronca, D. Romano, G. Forte, and E. Andablo-Reyes, *Adv. Polym. Technol.* 31, 193 (2012).
6. D. Romano, N. Tops, E. Andablo-Reyes, S. Ronca, and S. Rastogi, *Macromolecules* 47, 4750 (2014).
7. N. I. Ivancheva, S. N. Chvalun, S. S. Ivanchev, A. N. Ozerin, N. F. Bakeev, N. F. Eremeeva, D. A. Nikolaev, D. A. Pakhomov, I. V. Oleinik, and N. F. Tolstikov, RF Patent No. 2459835 S2, *Byull. Izobret.* No. 24 (2012).
8. S. S. Ivanchev, A. N. Ozerin, N. I. Ivancheva, S. N. Chvalun, I. I. Oleinik, N. F. Bakeev, M. G. Eremeeva, E. V. Sviridova, V. A. Aulov, I. V. Oleinik, and A. S. Keчек'yan, RF Patent No. 2552636 S2, *Byull. Izobret.* No. 16 (2015).
9. A. N. Ozerin, S. S. Ivanchev, S. N. Chvalun, V. A. Aulov, N. I. Ivancheva, and N. F. Bakeev, *Polymer Sci. Ser. A* 54, 950 (2012).
10. L. P. Myansikova, Yu. M. Boiko, V. M. Egorov, E.M. Ivan'kova, D. V. Lebedev, V. A. Marikhin, E. I. Radovanova, G. H. Michler, V. Seidewitz, and S. Goerlitz, in *Reactor Powder Morphology* (Nova Science, New York, 2011), Chap. 5.
11. M. V. Baidakova, P. V. Dorovatovskii, Ya. V. Zubavichus, E. M. Ivan'kova, S. S. Ivanchev, V. A. Marikhin, L. P. Myasnikova, and M. A. Yagovkina, *Phys. Solid State* 60, 897 (2018).
<https://doi.org/10.1134/S1063783418090044>
12. V. A. Aulov, M. A. Shcherbina, S. N. Chvalun, S. V. Makarov, I. O. Kuchkina, A. A. Pantyukhin, N. F. Bakeev, and Yu. S. Pavlov, *Polymer Sci., Ser. A* 46, 620 (2004).
13. Y. L. Yoo, O. H. Han, H.-K. Lee, and J. K. Song, *Polymer* 41, 1355 (2000).

[https://doi.org/10.1016/S0032-3861\(99\)00272-4](https://doi.org/10.1016/S0032-3861(99)00272-4)

14. L. P. Myasnikova, M. V. Baidakova, V. F. Drobot'ko, S. S. Ivanchev, E. M. Ivan'kova, E. I. Radovanova, M. A. Yagovkina, V. A. Marikhin, Y. V. Zubavichus, and P. V. Dorovatovskii, *J. Macromol. Sci. B* 58, 847 (2019).

<https://doi.org/10.1080/00222348.2019.1654692>

15. D. V. Lebedev, V. A. Marikhin, L. P. Myasnikova, P. N. Yakushev, and E. M. Ivankova, *J. Macromol. Sci. B* 52, 1770 (2013).

16. A. P. Melnikov, M. Rosenthal, A. I. Rodygin, D. Doblas, D. V. Anokhin, M. Burghammer, and D. A. Ivanov, *Eur. Polym. J.* 81, 598 (2016).

<https://doi.org/10.1016/j.eurpolymj.2015.12.031>

17. D. Ivanov, M. Rosenthal, A. Melnikov, A. Rychkov, D. Doblas, D. Anokhin, and M. Burghammer, in *Fast Scanning Calorimetry*, Ed. by V. B. F. Mathot and C. Schick (Springer Int., Switzerland, 2016), Chap. 9.

18. A. P. Melnikov, M. Rosenthal, and D. A. Ivanov, *ACS Macro Lett.* 7, 1426 (2018).

<https://doi.org/10.1021/acsmacrolett.8b00754>

19. S. S. Ivanchev, E. I. Ruppel', and A. N. Ozerin, *Dokl. Phys. Chem.* 468, 89 (2016).

20. T. Seto, T. Hara, and K. Tanaka, *Jpn. J. Appl. Phys.* 7, 31 (1968).

21. C. W. Bunn, *Trans. Faraday Soc.* 35, 482 (1939).

22. T. Kanaya and K. Kaj, in *High-Performance and Specialty Fibers: Concepts, Technology and Modern Application of Man-Made Fibers for the Future* (*Jpn. Soc. Fiber Sci. Technol.*, 2016), p. 16.

23. V. A. Berstein, V. M. Egorov, V. A. Marikhin, and L. P. Myasnikova, *Vysokomol. Soedin., Ser. A* 27, 771 (1985).

24. V. A. Berstein and V. M. Egorov, *Differential Scanning Calorimetry of Polymers* (Ellis Hoorwood, New York, 1994).

25. D. T. Grubb and M. J. Hill, *J. Cryst. Growth* 48, 321 (1980).

[https://doi.org/10.1016/0022-0248\(80\)90219-5](https://doi.org/10.1016/0022-0248(80)90219-5)

26. *Crystallization in Multiphase Polymer Systems*, Ed. By S. Thomas, A. P. Mohammed, E. B. Gowd, and N. Kalarikkal (Elsevier, Amsterdam, 2018).

27. V. M. Egorov, V. A. Marikhin, L. P. Myasnikova, A. K. Borisov, E. M. Ivan'kova, and S. S. Ivanchev, *Phys. Solid State* 61, 1927 (2019).